

## Alkyl chain substituted 1,9-pyrazoloanthrones exhibit prominent inhibitory effect on c-Jun N-terminal kinase (JNK)<sup>†</sup>

Cite this: *Org. Biomol. Chem.*, 2014, **12**, 4656

Karothu Durga Prasad,<sup>a</sup> Jamma Trinath,<sup>b</sup> Ansuman Biswas,<sup>c</sup> Kanagaraj Sekar,<sup>\*d</sup> Kithiganahalli N. Balaji<sup>\*b</sup> and Tayur N. Guru Row<sup>\*a</sup>

*N*-Alkyl substituted pyrazoloanthrone derivatives were synthesized, characterized and tested for their *in vitro* inhibitory activity over c-Jun N-terminal kinase (JNK). Among the tested molecules, a few derivatives showed significant inhibitory activity against JNK with minimal off-target effect on other mitogen-activated protein kinase (MAP kinase) family members such as MEK1/2 and MKK3,6. These results suggested that *N*-alkyl (propyl and butyl) bearing pyrazoloanthrone scaffolds provide promising therapeutic inhibitors for JNK in regulating inflammation associated disorders.

Received 12th March 2014,  
Accepted 2nd May 2014

DOI: 10.1039/c4ob00548a

www.rsc.org/obc

### 1. Introduction

Cellular physiological processes are critically tailored by numerous signalling pathways. Regulated activation of Mitogen Activated Protein Kinase (MAP kinase) family members determine the extent of mammalian gene expression.<sup>1</sup> Lipopolysaccharide (LPS), chief constituent of endotoxin, is the major cause of sepsis. Endotoxin mediated septic shock is mainly characterised by drastic and sudden augmentation of several inflammatory genes like IL-12, IL-1 $\beta$ , and TNF- $\alpha$ .<sup>2</sup> Exaggerated levels of these cytokines derails the host immune homeostasis, leading to inflammation associated risks like cardiac arrest, arthritis, *etc.*<sup>3</sup> Activation of the host cellular signalling pathways comprised of MAP kinases such as ERK1/2, p38 and JNK predominantly at the ground level is the key regulatory step in fine-tuning the immune cell associated functions.<sup>4,5</sup> Design and characterization of novel small molecules on the one hand and potentiating the exiting target specific inhibitors on the other attain crucial importance in the treatment of inflammation associated

disorders.<sup>6–8</sup> JNK (Jun N-terminal kinase), a stress activated protein kinase (SAPK), is one of the important members of the MAP kinase family along with MEK1/2, MEK3,6, MKK4,7, *etc.* that mediates the activation of the key transcription factor AP-1 (Activator Protein-1 complex composed of c-Fos and c-Jun).<sup>9–13</sup> Activated JNK phosphorylates c-Jun at the Ser63 position and eventually leads to formation of a functional AP-1 transcription factor complex.<sup>14,15</sup> To date, three JNKs were identified in humans (JNK1, JNK2 and JNK3). In addition to these, 10 subsidiary isoforms arise from these JNKs as splice variants.<sup>16</sup> JNKs with several isoformic variants control crucial cellular processes like apoptosis and cell proliferation and are also implicated in disorders associated with inflammation like septic shock, arthritis, inflammatory bowel disease, *etc.*<sup>17,18</sup> Therapeutic inhibition of JNK activity by small molecule inhibitors has proven to be advantageous in the treatment of diseases coupled with derailed inflammation.<sup>19,20</sup>

Even though several inhibitors of JNK have already been reported<sup>21–23</sup> with varied efficacies, the role of anthracyclines identified in the screening of anti-cancer drugs<sup>24</sup> had not been focused in terms of kinase inhibitors until the introduction of 1,9-pyrazoloanthrone (SP600125) by Brydon *et al.*<sup>19</sup> SP600125, a flat molecule<sup>25</sup> with a free NH group in the pyrazole ring, acts as a reversible ATP competitive inhibitor and has proved to be a small molecule inhibitor of JNK among several tested kinases.<sup>26–28</sup> But the methyl and ethyl derivatives of pyrazoloanthrone exhibited loss of inhibitory activity<sup>19</sup> and hence other higher alkyl derivatives were not tested. From a chemistry perspective, the tautomerism in 1,9-pyrazoloanthrone (anthra[1,9-*c,d*]pyrazol-6-one, Fig. 1a) was confirmed by the existence of two positional isomers after alkylation (Fig. 1b).<sup>29</sup> According to Scapin and co-workers,<sup>30</sup> the crystal structure of JNK3 with 1,9-pyrazoloanthrone (PDB code: 1PMV) showed

<sup>a</sup>Solid State and Structural Chemistry Unit, Indian Institute of Science, Bangalore, India. E-mail: sscnng@sscu.iisc.ernet.in; Fax: +91 80 23601310; Tel: +91 80 22932796

<sup>b</sup>Department of Microbiology and Cell Biology, Indian Institute of Science, Bangalore, India. E-mail: balaji@mcb.iisc.ernet.in; Fax: +91-80-23602697; Tel: +91-80-22933223

<sup>c</sup>Department of Physics, Indian Institute of Science, Bangalore, India

<sup>d</sup>Supercomputer Education and Research Centre, Indian Institute of Science, Bangalore, India

<sup>†</sup>Electronic supplementary information (ESI) available: Crystal structures, NMR and ligplots. CCDC SPE2-990062, SPP1-990060, SPP2-990061, SPB1-990059, SPB2-990535 and 983911. For ESI and crystallographic data in CIF or other electronic format see DOI: 10.1039/c4ob00548a

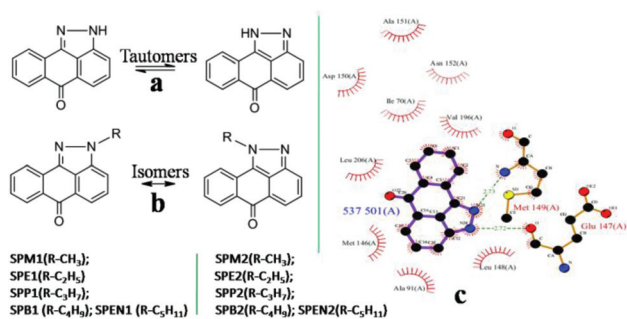


Fig. 1 Chemical structures of (a) 1,9-pyrazoloanthrone and (b) *N*-alkylated pyrazoloanthrones. (c) Ligplot representation of interactions in the active site of JNK3 with SP600125 (1PMV).

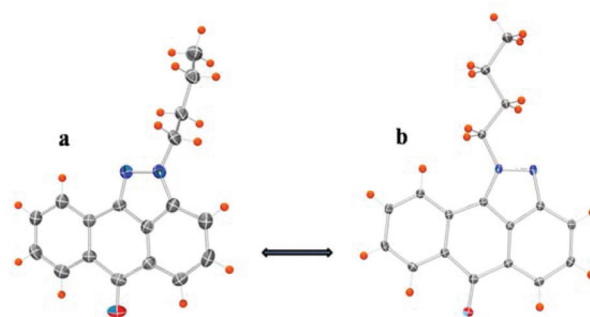


Fig. 2 ORTEP diagram of (a) SPB1 and (b) SPB2 with 50% probability displacement ellipsoids.

higher selectivity towards inhibition compared to the other molecules. It was shown that SP600125 interacts with the protein *via* hydrogen bonds with the carbonyl oxygen of Glu147 and the main chain nitrogen of Met149. In addition, several hydrophobic contacts with Ile70, Ala91, Met146, Leu148, Asp150, Asn152, Val196 and Leu206 (Fig. 1c) were identified in the enzyme–inhibitor complex.

In this context, it may be surmised that an increase in the alkyl chain length on the nitrogen atom might invoke additional hydrophobic contacts in the active site of JNK, a feature which needs to be explored. In the present study the tautomerism in 1,9-pyrazoloanthrone was substantiated by the positional isomers of alkyl derivatives and the structures have been established by single crystal X-ray diffraction studies. Based on calculated binding abilities with JNK structure generated from the *in silico* screening, 10 molecules were selected for initial screening of their kinase inhibitory activity. Among the tested molecules, a few of them show specific inhibition of JNK among the several MAP kinases with favourable concentrations in the range of 1–20  $\mu\text{M}$ . These molecules deserve further evaluation in terms of their pharmacokinetic properties as well as biological functions to be potent therapeutics in resolving inflammation.

## 2. Results and discussion

### 2.1. Synthesis

Based on preliminary results obtained with pyrazoloanthrones in *in silico* screening, *N*-alkyl substituted pyrazoloanthrones were synthesized according to modified procedures (ESI<sup>†</sup>). The compounds were characterized by <sup>1</sup>H & <sup>13</sup>C NMR, and HR-MS, and the purity was assessed by the analytical HPLC method and found to be >98%. The crystal structures of these compounds were determined by single crystal X-ray diffraction.

### 2.2. Crystal structure determination

Substitution of an alkyl group on the pyrazole ring in 1,9-pyrazoloanthrone forms two isomers. For example, two isomers of

Table 1 Crystallographic data for compounds SPB1 and SPB2

Compound	SPB1	SPB2
Formula	C <sub>18</sub> H <sub>16</sub> N <sub>2</sub> O	C <sub>18</sub> H <sub>16</sub> N <sub>2</sub> O
Formula weight	276.3324	276.3324
System	Orthorhombic	Monoclinic
Space group	<i>P</i> 2 <sub>1</sub> 2 <sub>1</sub> 2 <sub>1</sub>	<i>P</i> 2 <sub>1</sub> / <i>c</i>
<i>a</i> (Å)	4.909(5)	4.933(2)
<i>b</i> (Å)	14.694(2)	15.036(7)
<i>c</i> (Å)	19.031(2)	18.387(9)
$\alpha$	90	90
$\beta$	90	91.93(5)
$\gamma$	90	90
Volume (Å <sup>3</sup> )	1372.93(3)	1363.07(2)
<i>Z</i>	4	4
Density (g cm <sup>-3</sup> )	1.34	1.35
$\mu$ (mm <sup>-1</sup> )	0.084	0.085
<i>F</i> (000)	583.9	583.9
No. of measured reflections	9877	21 681
No. of unique reflections	3001	2671
No. of reflections used	1861	2173
<i>R</i> <sub>all</sub> , <i>R</i> <sub>obs</sub>	0.120, 0.067	0.058, 0.045
<i>wR</i> <sub>2-all</sub> , <i>wR</i> <sub>2-obs</sub>	0.193, 0.152	0.109, 0.102
$\Delta\rho_{\text{min,max}}$ (e Å <sup>-3</sup> )	-0.216, 0.257	-0.226, 0.234

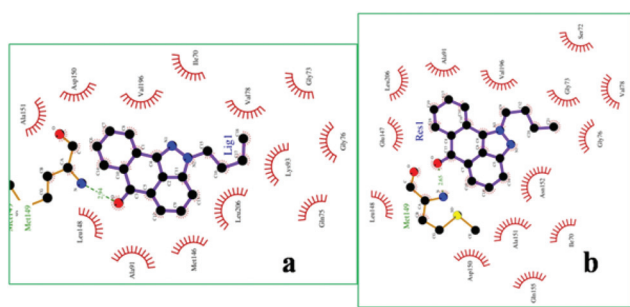
the butyl derivative of 1,9-pyrazoloanthrone (designated as SPB1 and SPB2) were crystallized from a mixture of 30% EtOAc–hexane and their crystal structures were determined (Fig. 2; Table 1). Similarly, several alkyl derivatives of pyrazoloanthrone (SPM1, SPE2, SPP1 and SPP2; ESI<sup>†</sup>) were crystallized by slow evaporation at ambient temperatures and their crystal structures were determined.

### 2.3. Virtual screening

The binding efficiencies of the alkyl derivatives were tested *in silico* using docking simulations around the active site of the protein. The known inhibitor SP600125 (537) was docked into the active site of JNK3 to obtain an estimate of its binding energy (−8.05 kcal mol<sup>-1</sup>). The predicted binding energies of the other molecules (listed in Table 2 according to increasing length of the alkyl group) were compared with this value. Compared to SP600125, all the derivatives, except SPM1 and SPE2, showed enhanced hydrophobic contacts. With the increase in

Table 2 Binding energies of 1,9-pyrazoloanthrone derivatives

Protein	Ligand	Binding energy (kcal mol <sup>-1</sup> )	Hydrogen bond between protein atom and ligand atom	No. of hydrophobic contacts
1PMV	537	-8.05	Met149 N...N Glu147 O...N	9
	<b>SP600125</b>			
	<b>SPM1</b>	-7.70	Met149 N...O	7
	<b>SPM2</b>	-7.80	Met149 N...O	11
	<b>SPE1</b>	-7.87	Met149 N...O	9
	<b>SPE2</b>	-7.90	Met149 N...O	11
	<b>SPP1</b>	-7.88	Met149 N...O	11
	<b>SPP2</b>	-8.09	Met149 N...O	13
	<b>SPB1</b>	-8.11	Met149 N...O	13
	<b>SPB2</b>	-8.27	Met149 N...O	14
	<b>SPEN1</b>	-8.61	Met149 N...O	11
	<b>SPEN2</b>	-8.69	Met149 N...O	13

Fig. 3 Ligplot representation of interactions in active site of JNK3 with (a) **SPB1** and (b) **SPB2**.

length of the substituting alkyl group, improved binding energies were observed. It is of interest to note that the binding energies of **SPB1** and **SPB2** are comparable to those of the parent compound and are enhanced in the case of **SPEN1** and **SPEN2** respectively.

As described in Fig. 1b the parent molecule 1,9-pyrazoloanthrone in the protein-inhibitor complex interacts with the protein *via* hydrogen bonds involving the carbonyl oxygen of Glu147 and the main chain nitrogen of Met149. The second hydrogen bonding is conserved in the interactions of all the *N*-alkylated pyrazoloanthrones (ESI<sup>†</sup>) with the JNK protein (1PMV), as observed from the docking simulations. Fig. 3a and 3b show the binding characteristics of **SPB1** and **SPB2** with conserved hydrogen bonding involving MET149. The Ligplot representations of interactions of the other derivatives are presented in ESI<sup>†</sup>.

## 2.4. Biological activity

**2.4.1. Evaluation of the biological efficacies of alkyl substituted pyrazoloanthrones.** Sometimes the inhibitor activity of compounds could also be a result of their toxic effects and consequently might cause a flawed conclusion. Hence, prior to utilization of these small molecules as inhibitors, the cytotoxic effect of these on macrophages at various concentrations has

been analyzed by MTT (3-(4,5-dimethylthiazol-2-yl)-2,5-diphenyltetrazolium bromide) assays. All the tested small molecules exhibited cytotoxic effects greater than 20–30% only beyond 30  $\mu$ M concentration (Fig. 4). DMSO is utilized in the study as a solvent control as it shows no significant cytotoxic effect and helps in confirming the specificity of the alkyl derivatives of 1,9-pyrazoloanthrone in dampening the cell survival. Based on these results, the maximum concentration of the pyrazoloanthrone derivatives that can be tested for target specific inhibition of JNK has been narrowed down to a range of 1  $\mu$ M to 30  $\mu$ M in further studies.

The kinase inhibitory effect of alkyl substituted pyrazoloanthrones was studied by monitoring the phosphorylation of c-Jun, an immediate downstream target of activated JNK in macrophages by the immunoblotting technique. All the alkyl substituted derivatives of pyrazoloanthrone exhibited the inhibition of JNK over a range of concentrations tested in LPS activated mouse macrophages. Of the compounds tested, **SPP1**, **SPB1** and **SPEN1** (propyl, butyl and pentyl derivatives of pyrazoloanthrone) demonstrated the inhibition of JNK at lower concentrations ranging from 1  $\mu$ M to 5  $\mu$ M whereas 1,9-pyrazoloanthrone showed inhibition with the minimum requirement of 10  $\mu$ M in LPS activated macrophages as shown in Fig. 5D–F and H respectively. As reported by Brydon *et al.*, the methyl and ethyl derivatives of pyrazoloanthrone showed significant loss in inhibitory activity;<sup>19</sup> however, compounds with propyl and butyl substitutions (**SPP1**, **SPB1** and **SPB2**) showed significant inhibitory function starting from 1  $\mu$ M whereas **SPEN1** showed inhibition from 5  $\mu$ M onwards. Intriguingly, all these obtained concentrations after the initial screen are far lower as compared to 1,9-pyrazoloanthrone which initiates inhibition only beyond 10  $\mu$ M (Fig. 5H).

Thus, the fact that the substitution of alkyl chains of increasing length enhances the hydrophobic interaction potential is quite evident from the extent of inhibitory activity with **SPP1**  $\approx$  **SPB1** > **SPEN1** > **SPM1** > **SPE1**. On the other hand, pyrazoloanthrone isomers (derivatives with alkyl substituents on the left side of the pyrazole ring) such as **SPP2** (5  $\mu$ M) and **SPB2** (1  $\mu$ M) also showed significant inhibition of JNK activity as well as phosphorylation of c-Jun in comparison with 1,9-pyrazoloanthrone. It is noteworthy that on further extension of chain length like in the case of the pentyl derivative of 1,9-pyrazoloanthrone, there is a sudden drop in the inhibitory activity and this may be attributed to the requirements of conserved hydrogen bonding at the binding site as demonstrated by the auto dock studies. Interestingly, **SPP1** and **SPB1** exhibited the inhibitory effect at a concentration lower than 1,9-pyrazoloanthrone.

In order to evaluate the specific inhibitory activity of **SPB1** and **SPP1** molecules over JNK compared to LPS induced activation of other MAP kinases such as ERK1/2 and p38, immunoblot analysis of the active state of ERK1/2 and p38 was carried out. **SPP1** and **SPB1** block LPS induced activation of ERK1/2 and p38 only at concentrations beyond 30  $\mu$ M with marginal off target effects (Fig. 6). These results suggest that alkyl substituted pyrazoloanthrone scaffolds need to be further

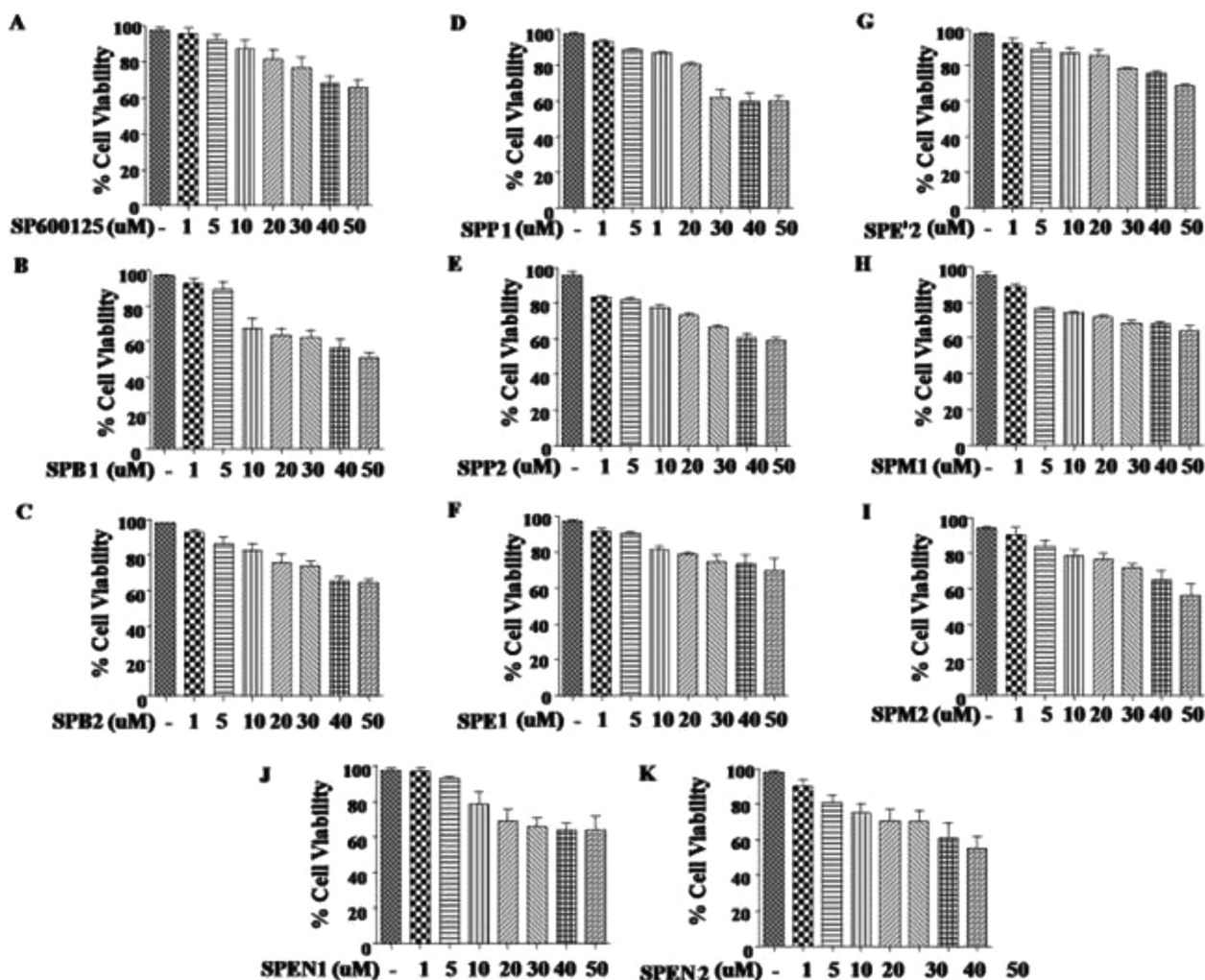


Fig. 4 Analysis of cytotoxic effect of small molecules by the MTT assay. Mouse peritoneal macrophages were treated with respective molecules at various concentrations for 12 hours and cell viability was analyzed by the MTT assay.

explored to treat inflammatory disorders with higher specificity at lower concentrations.

### 3. Conclusions

In conclusion, the synthesis, isolation and structural determination of alkyl isomers of pyrazoloanthrone derivatives have been achieved. The minimum required inhibitory concentration of these small molecule inhibitors was found to be less than 10  $\mu\text{M}$  in comparison with 1,9-pyrazoloanthrone to inhibit JNK. The structural correlations appear to support the inhibitor evaluation. The alkyl substituted scaffolds lead to molecules with potent and selective inhibition of JNK. Critically, our lead candidates **SPP1** and **SPB1** display specific inhibition of JNK among other LPS activated MAP kinases like ERK1/2 and p38. Our results suggest that these two scaffolds of inhibitors **SPP1** and **SPB1** would be promising leads for the future development of more potent and selective inhibitors to treat disorders associated with inflammation.

## 4. Experimental section

### 4.1. Materials and methods

**Isolation of mouse peritoneal macrophages.** Macrophages utilized in the study were isolated from C57/BL6J mice. In brief, mice were intraperitoneally injected with thioglycolate (2 mL of 2X concentration per mice). After 4 days of injection, mice were sacrificed. Peritoneal cavities were flushed with ice cold PBS and centrifuged to obtain the macrophages. Thus, the obtained cells were resuspended in DMEM containing 10% FBS (Sigma Aldrich) and seeded for further experiments. The experiments with mouse macrophages were carried out after the approval from the Institutional Ethics Committee for animal experimentation as well as from the Institutional Biosafety Committee.

### 4.2. Cell viability assay

Mouse macrophages were seeded in 96 well plates (75 000 cells per well) in 200  $\mu\text{l}$  of DMEM complete medium and incubated

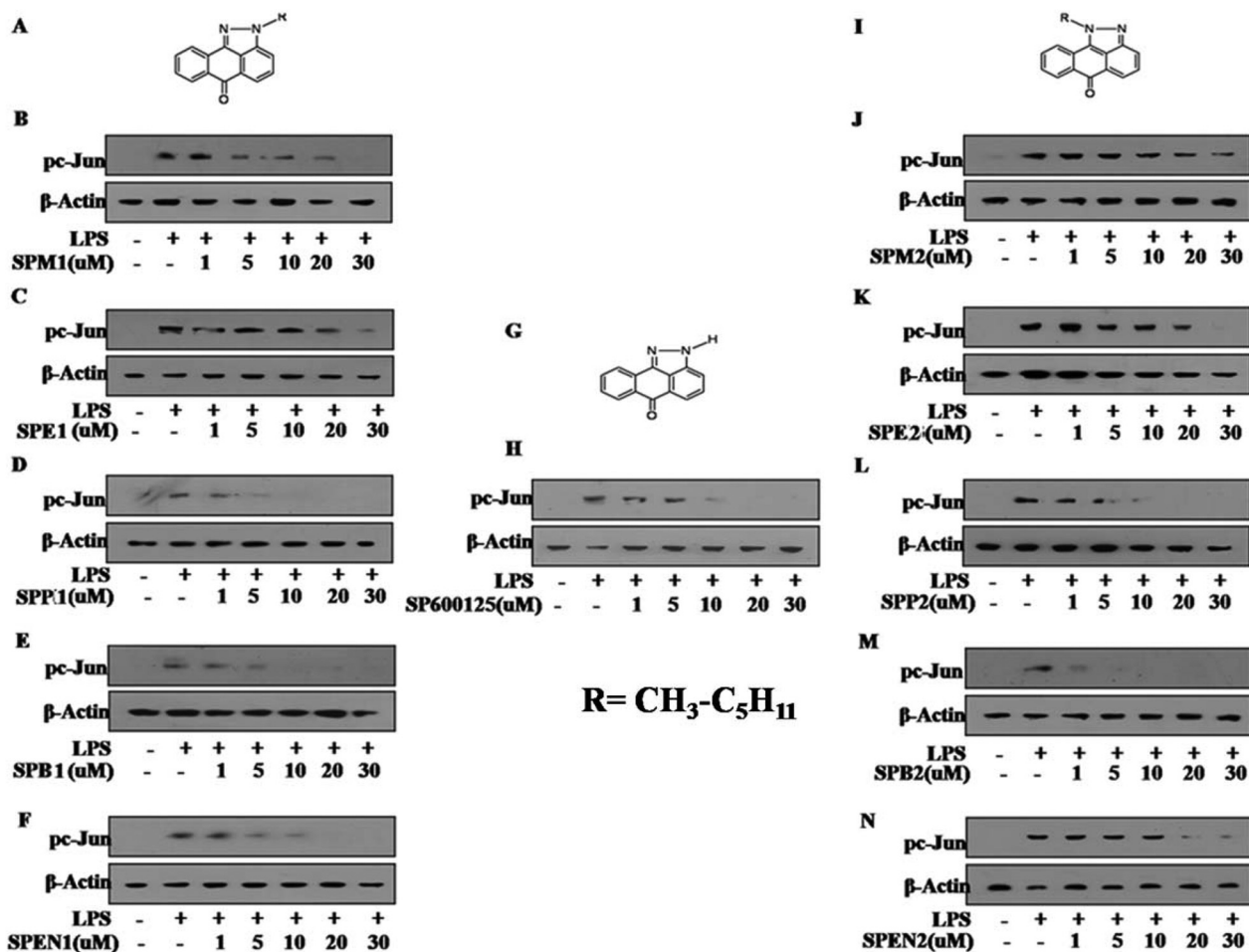


Fig. 5 Optimum inhibitory concentrations of 1,9-pyrazoloanthrone derivatives over phosphorylation of c-Jun. B–F and J–N show the immunoblots for phospho c-Jun in LPS (100 ng ml<sup>-1</sup>) activated macrophages at different concentrations of inhibitors tested. A, G and I represent the structures of 1,9-pyrazoloanthrone and its derivatives.

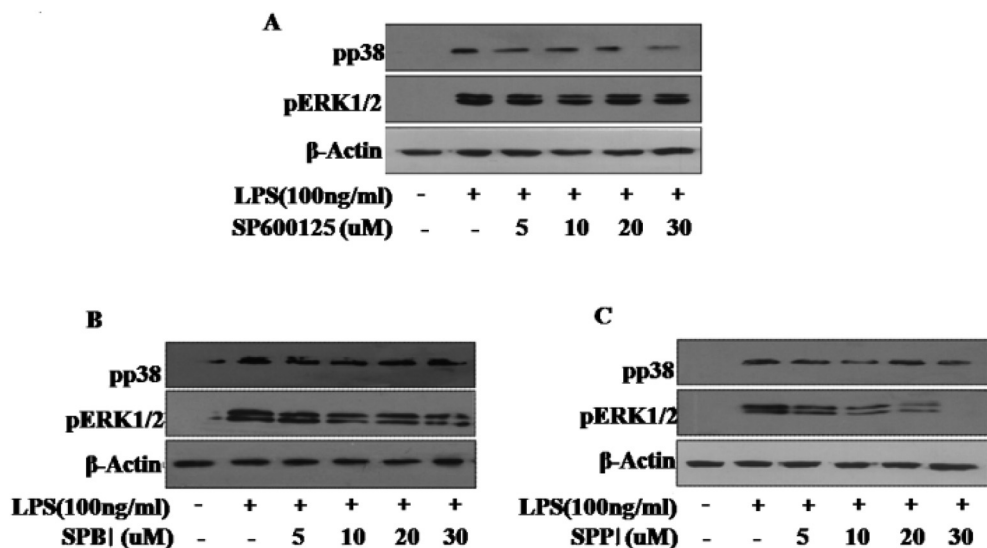


Fig. 6 Elucidation of the off-target effect of SPB1 and SPP1 over LPS induced MAP kinase activation. (A, B and C) Immunoblot analysis of LPS induced activation of p38, ERK1/2 in the presence of various concentrations of SP600125, SPB1 and SPP1 respectively in mouse macrophages.

overnight. Later, the cells were treated with small molecules reconstituted in DMSO at various concentrations as mentioned for 12 hours. Post 12 hour treatment, the medium was removed carefully and fresh medium (100  $\mu\text{l}$  per well) was added. 20  $\mu\text{l}$  of 5  $\text{mg ml}^{-1}$  of MTT reagent was added to each well and incubated for 4 hours at 37  $^{\circ}\text{C}$  aseptically. The medium was removed and DMSO (100  $\mu\text{l}$  per well) was added to the cells and left on an orbital shaker (150 rpm) for 15 min. After incubation, absorbance was read at 590 nm. Untreated cells served as the control in all the cell viability assays.

#### 4.3. Treatment with small molecule inhibitors

All the small molecules utilized in the study were reconstituted in sterile DMSO (Sigma-Aldrich, USA) and used at various concentrations as mentioned. DMSO at 0.1% concentration was used as the vehicle control. In all experiments with inhibitors, a tested concentration was used after careful titration experiments assessing the viability of the macrophages using the MTT assay. In experiments with inhibitors, the cells ( $4 \times 10^6$  per well) were treated with a given inhibitor for 60 min before experimental treatment.

#### 4.4. Immunoblotting

Macrophages were treated with respective small molecule inhibitors as mentioned and then stimulated with LPS (Sigma-Aldrich, USA), 100  $\text{ng ml}^{-1}$ , for an additional 60 min. Cells were washed twice with PBS, scrapped off the culture dish and collected by centrifugation. Cell lysates were prepared in RIPA buffer constituting 50 mM Tris-HCl (pH 7.4), 1% NP-40, 0.25% sodium deoxycholate, 150 mM NaCl, 1 mM EDTA, 1 mM PMSF, 1  $\mu\text{g ml}^{-1}$  of each aprotinin, leupeptin, pepstatin, 1 mM  $\text{Na}_3\text{VO}_4$ , and 1 mM NaF and incubated in ice for 30 min. Whole cell lysates were collected by centrifuging lysed cells at 13 000 rpm for 10 min at 4  $^{\circ}\text{C}$ . Equal amounts of protein from each cell lysate were subjected to SDS-PAGE and transferred onto PVDF membranes (Millipore, USA) by the semidry western blotting (Bio-Rad, USA) method. Nonspecific binding was blocked with 5% nonfat dry milk powder in TBST (20 mM Tris-HCl (pH 7.4), 137 mM NaCl, and 0.1% Tween 20) for 60 min. The blots were probed with anti-phospho Ser63 c-Jun for 12 hours at 4  $^{\circ}\text{C}$  and then washed with TBST thrice followed by anti-rabbit IgG HRP conjugated secondary antibody for 2 hours at 4  $^{\circ}\text{C}$ . Blots were washed and developed using the enhanced chemiluminescence detection system (Perkin Elmer, USA) as per the manufacturer's instructions. Blots were probed with anti- $\beta$ -actin HRP (Sigma-Aldrich, USA) to ensure equal loading of protein.

#### 4.5. Docking

The three-dimensional (3D) structures of all ten small molecules were modelled and minimised using the PRODRG server<sup>31</sup> and single crystal structures. AutoDock (version 4.2)<sup>32</sup> was used for the ligand-protein docking. The Lamarckian Genetic Algorithm was used with a population of 200 dockings. The docking output was analysed using Pymol and Ligplot.<sup>33</sup> Hydrogen bonds were determined using the in-built

HBPLUS<sup>34</sup> module in Ligplot with hydrogen bonding parameters ( $\text{D}\cdots\text{A}$  distance  $\leq 3.35$   $\text{\AA}$ ,  $\text{H}\cdots\text{A}$   $\leq 2.7$   $\text{\AA}$ ).

## Abbreviations

c-JNK	c-Jun N-terminal kinase
MAP Kinase	Mitogen activated protein kinase
LPS	Lipopolysaccharide
ERKs	Extracellular signal-regulated kinases

## Acknowledgements

Authors thank the Indian Institute of Science for infrastructure facilities and financial support. We thank the Central Animal facility, Indian Institute of Science for providing mice for experimentation. KDP and JT acknowledge fellowships from CSIR (Council of Scientific Industrial Research). TNG thanks DST for a J C Bose fellowship.

## References

- 1 D. C. Angus and T. V. Poll, *N. Engl. J. Med.*, 2013, **369**, 2062–2063.
- 2 N. A. Ali, *Crit. Care*, 2010, **14**, 160.
- 3 J. Moreira, *N. Engl. J. Med.*, 2013, **369**, 2062–2063.
- 4 W. J. Lin and W. C. Yeh, *Shock*, 2005, **24**, 206–209.
- 5 N. Mukaida, Y. Ishikawa, N. Ikeda, N. Fujioka, S. Watanabe, K. Kuno and K. Matsushima, *J. Leukoc. Biol.*, 1996, **59**, 145–151.
- 6 K. Watanabe, H. Nakagawa and S. Tsurufuji, *Agents Actions*, 1986, **17**, 472–477.
- 7 R. M. Pinheiro and J. B. Calixto, *Inflamm. Res.*, 2002, **51**, 603–610.
- 8 M. S. Inayat, I. S. El-Amouri, M. Bani-Ahmad, H. L. Elford, V. S. Gallicchio and O. R. Oakley, *J. Inflamm.*, 2013, **7**, 43.
- 9 T. Kallunki, B. Su, I. Tsigelny, H. K. Sluss, B. Derijard, G. Moore, R. Davis and M. Karin, *Genes Dev.*, 1994, **8**, 2996–3007.
- 10 B. Derijard, M. Hibi, I. H. Wu, T. Barrett, B. Su, T. Deng, M. Karin and R. J. Davis, *Cell*, 1994, **76**, 1025–1037.
- 11 M. A. Bogoyevitch and P. G. Arthur, *Biochim. Biophys. Acta*, 2008, **1784**, 76–93.
- 12 M. Karin, *J. Biol. Chem.*, 1995, **270**, 16483–6.
- 13 G. McMahon, L. Sun, C. Liang and C. Tang, *Curr. Opin. Drug Discov. Devel.*, 1998, **1**, 131–146.
- 14 V. C. Foletta, D. H. Segal and D. R. Cohen, *J. Leukoc. Biol.*, 1998, **63**, 139–152.
- 15 J. Jain, V. E. Valge-Archer and A. Rao, *J. Immunol.*, 1992, **148**, 1240–1250.
- 16 S. Gupta, T. Barrett, A. J. Whitmarsh, J. Cavanagh, H. K. Sluss, B. Derijard and R. J. Davis, *EMBO J.*, 1996, **15**, 2760–2770.
- 17 P. P. Graczyk, *Future Med. Chem.*, 2013, **5**, 539–551.

- 18 Z. Xia, M. Dickens, J. Raingeaud, R. J. Davis and M. E. Greenberg, *Science*, 1995, **270**, 1326–1331.
- 19 B. L. Bennett, D. T. Sasaki, B. W. Murray, E. C. O'Leary, S. T. Sakata, W. Xu, J. C. Leisten, A. Motiwala, S. Pierce, Y. Satoh, S. S. Bhagwat, A. M. Manning and D. W. Anderson, *Proc. Natl. Acad. Sci. U. S. A.*, 2001, **98**, 13681–13686.
- 20 A. Cerbone, C. Toaldo, S. Pizzimenti, P. Pettazzoni, C. Dianzani, R. Minelli, E. Ciamporcero, G. Roma, M. U. Dianzani, R. Canaparo, C. Ferretti and G. Barrera, *PPAR Res.*, 2012, 269751.
- 21 T. Kamenecka, R. Jiang, X. Song, D. Duckett, W. Chen, Y. Y. Ling, J. Habel, J. D. Laughlin, J. Chambers, M. Figuera-Losada, M. D. Cameron, L. Lin, C. H. Ruiz and P. V. LoGrasso, *J. Med. Chem.*, 2010, **53**, 419–431.
- 22 N. Kwiatkowski, N. Jelluma, P. Filippakopoulos, M. Soundararajan, M. S. Manak, M. Kwon, H. G. Choi, T. Sim, Q. L. Deveraux, S. Rottmann, D. Pellman, J. V. Shah, G. J. Kops, S. Knapp and N. S. Gray, *Nat. Chem. Biol.*, 2010, **6**, 359–368.
- 23 M. A. Siddiqui and P. A. Reddy, *J. Med. Chem.*, 2010, **53**, 3005–3012.
- 24 H. D. Showalter, J. L. Johnson, J. M. Hoftiezer, W. R. Turner, L. M. Werbel, W. R. Leopold, J. L. Shillis, R. C. Jackson and E. F. Elslager, *J. Med. Chem.*, 1987, **30**, 121–131.
- 25 K. D. Prasad, N. Venkataramaiah and T. N. Guru Row, *Cryst. Growth Des.*, 2014, **14**, 2118–2122.
- 26 K. Assi, R. Pillai, A. Gomez-Munoz, D. Owen and B. Salh, *Immunology*, 2006, **118**, 112–121.
- 27 Y. T. Ip and R. J. Davis, *Curr. Opin. Cell Biol.*, 1998, **10**, 205–219.
- 28 N. Miyakoshi, C. Richman, Y. Kasukawa, T. A. Linkhart, D. J. Baylink and S. Mohan, *J. Clin. Invest.*, 2001, **107**, 73–81.
- 29 L. Havlíčková, A. Koloničný, A. Lyčka, J. Jirman and I. Kolb, *Dyes Pigm.*, 1989, **10**, 1–11.
- 30 G. Scapin, S. B. Patel, J. Lisnock, J. W. Becker and P. V. LoGrasso, *Chem. Biol.*, 2003, **10**, 705–712.
- 31 A. W. Schuttelkopf and D. M. F. Van Aalten, PRODRG - a tool for high-throughput crystallography of protein-ligand complexes, *Acta Crystallogr., Sect. D: Biol. Crystallogr.*, 2004, **60**, 1355–1363.
- 32 G. M. Morris, R. Huey, W. Lindstrom, M. F. Sanner, R. K. Belew, D. S. Goodsell and A. J. Olson, AutoDock4 and AutoDockTools4: automated docking with selective receptor flexibility, *J. Comput. Chem.*, 2009, 2785–2791.
- 33 A. C. Wallace, R. A. Laskowski and J. M. Thornton, LIGPLOT: A program to generate schematic diagrams of protein-ligand interactions, *Prot. Eng.*, 1995, **8**, 127–134.
- 34 I. K. McDonald and J. M. Thornton, *J. Mol. Biol.*, 1994, **238**, 777–793.